

Model-mapped random phase approximation to evaluate superconductivity in the fluctuation exchange approximation from first principles

Hirofumi Sakakibara^{1,2*} and Takao Kotani¹

¹*Department of applied mathematics and physics, Tottori university, Tottori 680-8552, Japan and*

²*Computational Condensed Matter Physics Laboratory, RIKEN, Wako, Saitama 351-0198, Japan*

(Dated: May 23, 2019)

We have applied the model-mapped RPA [H. Sakakibara *et al.*, J. Phys. Soc. Jpn. **86**, 044714 (2017)] to the cuprate superconductors La_2CuO_4 and $\text{HgBa}_2\text{CuO}_4$, resulting two-orbital Hubbard models. All the model parameters are determined based on first-principles calculations. For the model Hamiltonians, we perform fluctuation exchange calculation. Results explain relative height of T_c observed in experiment for La_2CuO_4 and $\text{HgBa}_2\text{CuO}_4$. In addition, we give some analyses for the interaction terms in the model, especially comparisons with those of the constrained RPA.

PACS numbers: 74.20.Pq, 74.72.-h, 71.15.-m

I. INTRODUCTION

It is not so easy to treat strongly-correlated electrons only by first-principles calculations. Thus we often use a procedure via a model Hamiltonian^{1,2}; we determine a model Hamiltonian \hat{H}_M from a first-principles calculation and then solve the model Hamiltonian. This is inevitable because first-principles calculations, which are mainly based on the density functional theory (DFT) in the local density approximation (LDA), are very limited to handle systems with correlated electrons. Widely used model Hamiltonians are the Hubbard ones, which consist of one-body Hamiltonian \hat{H}_M^0 and the on-site interactions \hat{U}_M . To solve the Hubbard models, we can use a variety of methods³⁻¹⁰ such as fluctuation exchange approximation (FLEX)¹¹.

To determine \hat{H}_M , we have formulated the model-mapped random phase approximation (mRPA) in Ref. 12 recently. In mRPA, we use the standard procedure of the maximally localized Wannier function^{13,14} to determine \hat{H}_M^0 . Here \hat{H}_M^0 is determined as a projection of the one-body Hamiltonian of first-principles onto a model space, which is spanned by the Wannier functions. Then we determine \hat{U}_M so that the screened interaction of the model in the random phase approximation (RPA) agrees with that of the first-principles. In this paper, we consider on-site-only interaction in the model. Then we determine one-body double-counting term \bar{U}_M . Finally we have $\hat{H}_M = \hat{H}_M^0 + \hat{U}_M - \bar{U}_M$.

mRPA can be taken as one of the improvements of cRPA^{15,16} in the sense to determine screened Coulomb interaction without screening effects from the model space. Until now, a variety of cRPA methods have been developed¹⁷⁻³⁶. For example, Şaşıoğlu, Freidlich and Blüegel^{23,32} developed a convenient cRPA method applicable to the case of entangled energy bands, while Miyake *et al.*¹⁹ treated the case in a different manner. Nomura *et al.* showed a method to estimate the effective interaction for impurity problems in DMFT²⁵. Casula *et al.* showed a method beyond the RPA to include the band renormalization effects²⁹.

In this paper, we apply mRPA to high- T_c cuprate superconductors La_2CuO_4 ($T_c = 39$ K [37], denoted by La) and $\text{HgBa}_2\text{CuO}_4$ ($T_c = 98$ K [38], denoted by Hg) to determine \hat{H}_M of a two-orbital model³⁹⁻⁴². After we determine \hat{H}_M , we perform FLEX calculations to investigate superconductivity. Our results are consistent with experiments. Since this mRPA+FLEX procedure can be performed without parameters by hand, we can claim that relative height of T_c among materials is evaluated just from crystal structures. Thus, in principle, mRPA+FLEX can be used to find out a highest T_c material among a lot of possible materials.

We like to emphasize importance of the two-orbital model³⁹⁻⁴². Although the Fermi surface of cuprates consists of the $d_{x^2-y^2}$ orbital mainly, Sakakibara *et al.* pointed out that hybridization of the $d_{x^2-y^2}$ orbital with the d_{z^2} orbital⁴³⁻⁴⁹ is very important. This can be represented by the two-orbital model. Sakakibara's FLEX calculation showed that the hybridization degrades spin-fluctuation-mediated superconductivity. This explains the difference of T_c between La and Hg cuprates³⁹. A recent photoemission experiment for La cuprate has captured significant orbital hybridization effects⁵⁰.

II. METHOD

Let us summarize the formulation of mRPA in Ref. 12. First of all, we have to parametrize the interaction \hat{U}_M of the model Hamiltonian so that \hat{U}_M is specified by finite numbers of parameters. Fig. 1 is a chart about how we determine \hat{H}_M . Step (1) is by first-principles calculations, and step (2), (3) are by model calculations. In this paper, we will treat the on-site-only interaction of the two-orbital model specified by four parameters.

In step (1) of Fig. 1, we first perform a self-consistent calculation in first-principles method. Then we can obtain one-body Hamiltonian \hat{H}_M^0 in the standard procedure of maximally localized Wannier function^{13,14}. In addition, we calculate static screened Coulomb interaction $W(\mathbf{r}, \mathbf{r}', \omega = 0)$ in RPA. Hereafter we omit $\omega = 0$

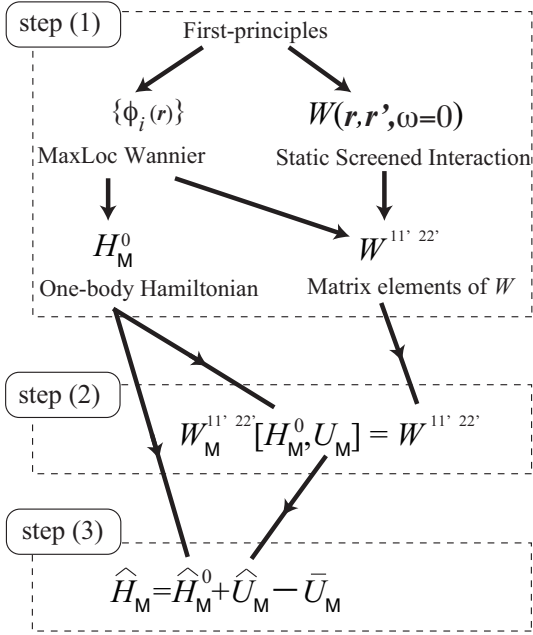


FIG. 1. How mRPA determines a model Hamiltonian \hat{H}_M . Note that quantities with subscript M are for the model Hamiltonian. At step (1), we obtain one-body Hamiltonian H_M^0 and RPA screened Coulomb interaction $W^{11'22'}$ in a first-principles calculation. At step (2), we obtain effective interaction U_M in the model, where we require $W_M^{11'22'}$ should be the same as $W^{11'22'}$. At step (3), we determine \bar{U}_M , which is to remove the double counting in the one-body term.

since we treat only the static case in this paper. Then we calculate matrix elements $W^{11'22'}$ of the matrix W , defined as

$$\begin{aligned} W^{11'22'} &= \langle 11' | W | 22' \rangle \\ &= \int d^3\mathbf{r} d^3\mathbf{r}' w_1^*(\mathbf{r}) w_1(\mathbf{r}) W(\mathbf{r}, \mathbf{r}') w_2^*(\mathbf{r}') w_2(\mathbf{r}'), \end{aligned} \quad (1)$$

where $\{w_1(\mathbf{r})\} = \{w_{i_1 \mathbf{R}_1}(\mathbf{r})\}$ are the Wannier functions. \mathbf{R} and i denote a position of primitive cell and an orbital in each cell, respectively. The number of elements $W_M^{11'22'}$ is the same as the number of elements $U_M^{11'22'}$. Calculations are performed with ecalj package available from Git-hub⁵³.

In step (2), we determine U_M , so that it satisfies

$$W_M^{11'22'}[H_M^0, U_M] = W^{11'22'}, \quad (2)$$

where a functional $W_M^{11'22'}[H_M^0, U_M]$ is a screened interaction in RPA calculated from H_M^0 and U_M . Here H_M^0 denotes the matrix whose elements are $H_M^{0,12}$; U_M denotes the matrix whose elements are $U_M^{11'22'}$ as well. \hat{H}_M^0 is the second quantized operator made of the matrix H_M^0 , \hat{U}_M as well. The functional is defined just in the model calculation; we do not treat quantities spatially dependent on \mathbf{r} . Eq. (2) is a key assumption of mRPA; we require that the screened interaction in a model should be the same as

those of theoretical correspondence in the first-principles calculation.

Let us detail the functional $W_M^{11'22'}[H_M^0, U_M]$. With non-interacting polarization function $P_M[H_M^0]$ of a model, we have effective interaction W_M in RPA as

$$W_M[H_M^0, U_M] = \frac{1}{1 - U_M P_M[H_M^0]} U_M. \quad (3)$$

Hereafter we omit H_M^0 in P_M for simplicity. Here we only treat non-magnetic case. From Eq. (3), we have

$$W_M^{i_1 i_1' i_2 i_2'}[H_M^0, U_M] = \frac{1}{N} \sum_{\mathbf{q}} \left[\frac{1}{1 - U_M P_M(\mathbf{q})} U_M \right]_{i_1 i_1' i_2 i_2'} \quad (4)$$

for on-site interactions U_M and W_M . Eq. (4) is used in Eq. (2) so as to determine U_M .

In step (3), we evaluate the one-body double counting term \bar{U}_M contained in the total model Hamiltonian \hat{H}_M . It is written as

$$\hat{H}_M = \hat{H}_M^0 + \hat{U}_M - \bar{U}_M. \quad (5)$$

To determine \bar{U}_M , we require that the contribution from \hat{U}_M and that from \bar{U}_M completely cancel when we treat \hat{U}_M in a mean-field approximation. The mean-field approximation should theoretically correspond to the first-principle method from which we start. For example, if we use quasi-particle self-consistent GW (QSGW)^{54–56} as the first-principle method, we have to use QSGW to treat the model of Eq. (5). Then \bar{U}_M is made of the Hartree term and the static self-energy term in the model. These terms cancel the effect of \hat{U}_M when QSGW is applied to. In this case, we have reasonable theoretical correspondence between the first-principle calculation and model calculation. However, if we use LDA as the first-principle method, we have no corresponding mean-field approximation. Thus we cannot uniquely determine \bar{U}_M . Instead of determining \bar{U}_M , we use a practical method to avoid double counting in FLEX (see Sec. IV).

Let us recall the procedure of cRPA as a reference to mRPA. The effective interaction of cRPA (U_m) is determined based on the requirement

$$\frac{1}{1 - vP} v = \frac{1}{1 - U_m P_m} U_m, \quad (6)$$

where $v(\mathbf{r}, \mathbf{r}')$ is the bare Coulomb interaction, $P_m(\mathbf{r}, \mathbf{r}')$ is the polarization function within the model space spanned by the maximally localized Wannier functions. Eq. (6) leads to

$$U_m = \frac{1}{1 - v(P - P_m)} v. \quad (7)$$

Then we calculate the on-site matrix elements $U_m^{122'1'}$ = $\langle 11' | U_m | 22' \rangle$.

Generally speaking, this cRPA procedures of Eq. (7) cannot be applicable to systems with entangled energy bands if the positive definiteness of $-(P - P_m)$ in Eq. (7) is not satisfied. In fact, we have checked that $-(P - P_m)$

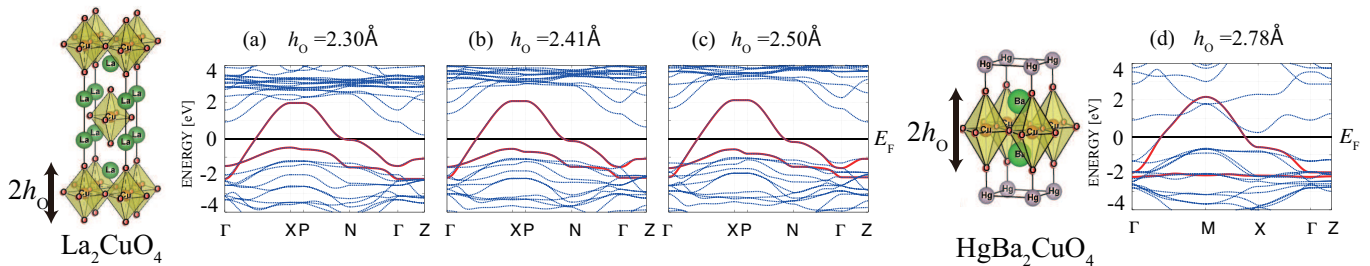


FIG. 2. (Color online) Crystal structures and band structures of La_2CuO_4 (a)-(c) and $\text{HgBa}_2\text{CuO}_4$ (d). Blue dashed lines are for the LDA band structures; red solid lines are for the two-orbital models. The cases (a)-(c) are for varying the apical oxygen height h_{O} . The cases (b) and (d) are with the experimental h_{O} ^{51,52}.

do not satisfy the positive definiteness for La and Hg. Thus we need to use a modified P_{m} satisfying the positive definiteness in a manner given by Şaşıoğlu, Freidlich and Blüegel^{23,32}. In their method, such P_{m} is given in Eq. (60) in Ref. 32 as

$$P_{\text{m}}(\mathbf{r}, \mathbf{r}') = \sum_i^{\text{occ}} \sum_j^{\text{unocc}} \frac{-2(c_i c_j)^2 \phi_i(\mathbf{r}) \phi_j^*(\mathbf{r}) \phi_j(\mathbf{r}') \phi_i^*(\mathbf{r}')}{\epsilon_j - \epsilon_i} \quad (8)$$

where ϕ_i is the eigenfunctions. The probability factor c_i is the norm for $\phi_i(\mathbf{r})$ projected into the model space spanned by the Wannier functions (See Eq. (58) in Ref. 32). The composite index $i = (\mathbf{k}, n)$ is for the wave number \mathbf{k} and the band index n . Apparently, $0 \leq c_{\mathbf{k}n} \leq 1$ and $\sum_n (c_{\mathbf{k}n})^2 = 1$ are satisfied for given \mathbf{k} . Thus $-(P - P_{\text{m}})$ is clearly positive definite because it is calculated just from the equation with $1 - (c_i c_j)^2$ instead of $-(c_i c_j)^2$ in the numerator of Eq. (8).

TABLE I. The interactions of mRPA (U_{M}) and cRPA (U_{m}) in a three-orbital model for SrVO_3 , where d_{xy} , d_{yz} , and d_{zx} orbitals are considered. U , U' , J are the intra-orbital, inter-orbital, and exchange interactions, respectively. The static screened interaction W is also shown in the same manner as U_{M} .

SrVO_3	mRPA		cRPA
[eV]	W	U_{M}	U_{m}
U	0.852	2.82	3.12
U'	0.248	1.88	2.17
J	0.290	0.442	0.448

As a check for our implementation of mRPA and cRPA, we show U_{m} and U_{M} for SrVO_3 where three $3d$ bands spanning model space are clearly separated from the other bands. In this case, we can expect that non-zero c_i are not widely distributed among energy bands. Only c_i for the three $3d$ bands are almost unity, while others are almost zero. In this case, as shown in Table I, U_{m} is close to U_{M} : U of U_{M} , 2.82 eV, is only a little smaller than U of U_{m} , 3.12 eV. This is reasonable since both mRPA and cRPA are to remove screening effect related to the model space, although we treat only the on-site interactions in mRPA. The difference $2.82 - 3.12 = -0.30$ eV

may be mainly explained by the effect of off-site interactions. To check this, we apply mRPA using Eq. (9) of Ref. 12 including the interactions between all vanadium sites. In this case, the values obtained in mRPA should be in agreement with that of cRPA in principle. We find that U of U_{M} become larger⁵⁷ to be 3.33 eV, slightly overshoots but becomes closer to 3.12 eV. Still remaining difference $3.33 - 3.12 = 0.21$ eV may be due to detailed differences of formalisms and numerical treatment.

III. RESULT FOR EFFECTIVE INTERACTION

Following the chart of Fig. 1, we apply mRPA to single-layered cuprates, La and Hg, to obtain the two-orbital Hubbard model³⁹, where we start from LDA calculations. We show their experimental crystal structures^{51,52} in Fig. 2, together with their LDA band structures in (b) and (d), where we superpose the energy bands of the two-orbital models. In addition, we treat hypothetical cases varying apical oxygen height h_{O} in La, (a) and (c), in order to clarify differences between mRPA and cRPA. Here h_{O} is defined as the distance shown in Fig. 2. The matrix U_{M} of the two-orbital model is represented as

$$U_{\text{M}} = \begin{pmatrix} U^{x^2-y^2} & 0 & 0 & U' \\ 0 & U^{J'} & U^J & 0 \\ 0 & U^J & U^{J'} & 0 \\ U' & 0 & 0 & U^{z^2} \end{pmatrix}, \quad (9)$$

where the indices of the matrix U_{M} takes $d_{x^2-y^2}d_{x^2-y^2}$, $d_{x^2-y^2}d_{z^2}$, $d_{z^2}d_{x^2-y^2}$, and $d_{z^2}d_{z^2}$. Here U' is inter-orbital Coulomb interactions; $U^J = U^{J'}$ are exchange interactions. Other interactions such as W_{M} are represented as well.

In Table II, we show values of U_{M} for La and Hg (Fig. 2(b) and 2(d)), together with values of W ⁵⁸. At first, let us compare W for La and Hg. We see a little difference on $W^{x^2-y^2}$ (0.747eV vs. 0.820 eV), while larger difference on W^{z^2} (1.58 eV vs. 3.83 eV). This is expected since Hg is more anisotropic than La, as indicated by the size of h_{O} . From these W and the band structure of the two-orbital model, we have obtained U_{M} shown in Table II.

TABLE II. The interactions of mRPA (U_M) and cRPA (U_m) for the experimentally observed crystal structure of La_2CuO_4 and $\text{HgBa}_2\text{CuO}_4$ ^{51,52}. The elements of W are defined in the same manner as U_M (see text).

La_2CuO_4		mRPA		cRPA
[eV]	W	U_M	U_m	
$U^{x^2-y^2}$	0.747	2.76	3.14	
U^{z^2}	1.58	2.63	2.95	
U'	0.370	1.64	2.01	
U^J	0.273	0.44	0.41	
$\text{HgBa}_2\text{CuO}_4$		mRPA		cRPA
[eV]	W	U_M	U_m	
$U^{x^2-y^2}$	0.820	2.99	2.14	
U^{z^2}	3.83	5.47	4.93	
U'	0.724	2.62	1.92	
U^J	0.460	0.67	0.58	

We see that ratios U_M/W are similar for La and Hg, that is, $2.76/0.747 \sim 2.99/0.820$ for $W^{x^2-y^2}$, other elements as well. This is consistent with the similarity of the band structure shown in Fig.2 (b) and (d).

We find that $U_M^{x^2-y^2}$ is roughly estimated by

$$U_M^{x^2-y^2} \sim \frac{W^{x^2-y^2}}{1 + W^{x^2-y^2} P_M^{x^2-y^2}}, \quad (10)$$

where $P_M^{x^2-y^2}$ is the diagonal elements of the Brillouin zone average of $P_M(\mathbf{q})$. Eq.(10) is derived from Eq.(4) by replacing $P_M(\mathbf{q})$ with the average. Let us evaluate Eq.(10). Our calculation gives $P_M^{x^2-y^2} = -0.97$ eV⁻¹ for La, -0.91 eV⁻¹ for Hg. The little difference $-0.06 = (-0.97) - (-0.91)$ eV⁻¹ corresponds to the little difference of the band structures of the two-orbital models shown in Fig. 2(b) and 2(d). Together with the values of $W^{x^2-y^2} = 0.747, 0.820$ eV in Table II, Eq.(10) gives $U_M^{x^2-y^2} \sim 2.71$ eV for La and ~ 3.23 eV for Hg. These are roughly in agreements with $U_M^{x^2-y^2} = 2.76$ and 2.99 eV in Table II. This analysis indicates that the difference of $U_M^{x^2-y^2}$ between La and Hg is mainly due to the difference of $W^{x^2-y^2}$.

In Table II, we also show cRPA values U_m for comparison. For La, Table II shows that U_m gives good agreement with U_M , a little smaller as in the case of SrVO_3 in Table I. On the other hand, we see large discrepancy for Hg : $U_m^{x^2-y^2} = 2.14$ eV is much smaller than $U_M^{x^2-y^2} = 2.99$ eV. This difference can be explained by Eq.(8) with factors c_i . In Hg, we see a stronger d - p hybridization in Fig.2 (d) than La; the position of $\text{Cu-}d_{x^2-y^2}$ band is pushed down to be in the middle of oxygen bands. This means that non-zero c_i are more distributed among the oxygen bands in the case of Hg than in the case of La. This can be a reason to make the effective size of P_m smaller than P_M in the case of Hg, resulting the smaller U_m .

To confirm the effect of hybridization, we calculate U_m and U_M by varying h_O for La. As discussed in Ref. 39, h_O

is a key quantity to determine the critical temperatures of superconductors⁵⁹⁻⁶⁴. We can see h_O works as a control parameter of hybridization^{34,63,64}. That is, as shown in 2(a)-(c), higher h_O pushes down $\text{Cu-}d_{x^2-y^2}$ levels more, resulting larger hybridization with oxygen bands. Fig. 2(d) for Hg can be taken as a case with highest h_O .

In Fig. 3, we plot U_M and U_m together with W . Let us focus on Fig. 3(a) and (e). As a function of h_O , $W^{x^2-y^2}$ is almost constant. In addition, the energy bands of the two-orbital model change little as shown in Fig. 2(a)-(c). Thus it is reasonable that $U_M^{x^2-y^2}$ changes little in Fig. 3(a), because of Eq.(10). On the other hand, $U_m^{x^2-y^2}$ decreases rapidly when h_O becomes higher. This means that P_m becomes smaller for higher h_O . As in the case of Hg case, we think this is because of larger hybridization of $\text{Cu-}d_{x^2-y^2}$ bands with oxygen bands.

Our mRPA and cRPA results are rather different. In Ref. 34, we treated a variety of layered cuprates, where we show that the effective interaction for La is larger than that for Hg as shown by U_m in Table II, based on the cRPA calculations. In addition, we showed the effective interactions are controlled by h_O as shown in U_m in Fig. 3. Even though we do not need to modify the overall conclusion in Ref. 34, we should not take such effective interactions as suitable for Hubbard models. Along the logic of mRPA, we should use U_M instead of U_m .

IV. FLEX CALCULATION FOR SUPERCONDUCTIVITY

For the model Hamiltonian \hat{H}_M obtained from mRPA, we perform two-orbital FLEX calculations to obtain dressed Green's functions $G_{ij}(k)$ ^{11,65-68}. Here $k = (\mathbf{k}, i\omega_n)$ is a composite index made of the wave vector \mathbf{k} and the Matsubara frequency $i\omega_n$. The band index i takes 1 or 2. We calculate only the optimally doped case for T_c (15% doping). We take $32 \times 32 \times 4$ k -meshes and 1024 Matsubara frequencies.

Let us remind step (3) in Fig. 1 to determine the counter one-body term \bar{U}_M . Instead of LDA, let us consider QSGW case first. Theoretically, it is easier since QSGW is a method directly applicable even to a model Hamiltonian, where QSGW determines a mean-field one-body Hamiltonian for the model. We first determine \hat{H}_M^0 in QSGW by the first-principle QSGW calculation and the Wannier function method in the step (1) of mRPA. Then we can determine \hat{U}_M in the step (2) of mRPA. In the step (3), we apply the QSGW method to the model Hamiltonian $\hat{H}_M = \hat{H}_M^0 + \hat{U}_M - \bar{U}_M$, where yet unknown term \bar{U}_M is included. Here \bar{U}_M is determined so that the QSGW applied to H_M do give the mean-field one-body Hamiltonian \hat{H}_M^0 . That is, the effect of \hat{U}_M to the one-body Hamiltonian is completely canceled by \bar{U}_M .

When we start from LDA instead of QSGW, we have no unique way to determine \bar{U}_M since LDA cannot be applicable to the model Hamiltonian. Thus we need some

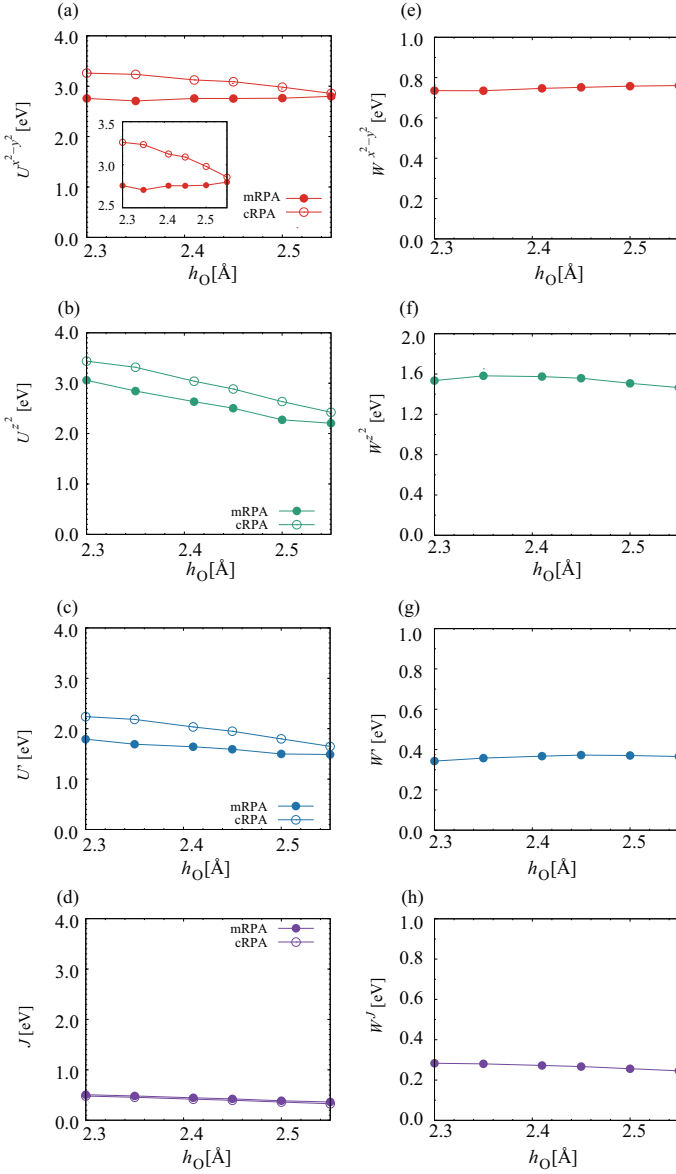


FIG. 3. (Color online) The elements of U_M (mRPA), U_m (cRPA), and W are plotted as a function of h_O . Details of numerical settings are shown in the text. Note that $W_M^{11'22'}[U_M] = W^{11'22'}$ is satisfied at any values of h_O . Panels (a) and (e) indicate that $U^{x^2-y^2}$ for cRPA is affected by the localization of Wannier functions (see text).

assumption to follow the case of QSGW. Here we identify the static part of the self-energy $\Sigma(\mathbf{k}, 0)$ as \bar{U}_M (our definition of $\Sigma(\mathbf{k}, 0)$ here includes the Hartree term). In other words, if we perform a static FLEX calculation with $\Sigma(\mathbf{k}, 0)$, we reproduce the one-body Hamiltonian of LDA. This method is equivalent to Eq. (5) in Ref. 69. We simply assume FLEX is not for the mean-field part, but for the ω -dependent self-energy part.

Here we investigate superconductivity in the two-orbital model. By substituting $G_{ij}(k)$ into the linearized

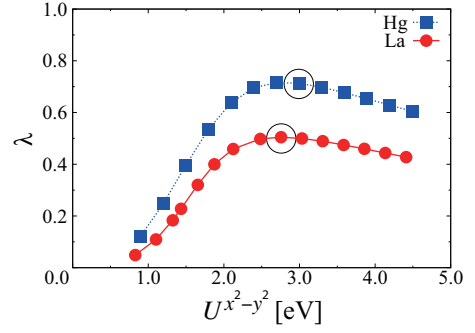


FIG. 4. (Color online) The eigenvalues λ of the Eliashberg equation are plotted as a function of $U^{x^2-y^2}$. Here the temperature is 0.01 eV. Red filled circles show the value for La and blue squares for Hg. Open circles indicate the results obtained with the value shown in table II.

Eliashberg equation,

$$\lambda \Delta_{ij}(k) = -\frac{T}{N} \sum_{q, m_i} V_{im_1 m_4 j}(q) G_{m_1 m_2}(k-q) \times \Delta_{m_2 m_3}(k-q) G_{m_4 m_3}(-k+q), \quad (11)$$

we obtain the gap function $\Delta_{ij}(k)$ as an eigenstate and its eigenvalue λ , where $V(q)$ is the singlet pairing interaction as described in Eq. (2)-(7) of Ref. 40. The largest λ reaches unity at $T = T_c$. Since λ is monotonic and increasing function of T^{-1} , we use λ at $T = 0.01$ eV as a qualitative measure of T_c instead of calculating at T_c . In some FLEX calculations, λ at fixed temperature is used to compare relative height of T_c among similar materials^{69,70}. We obtain $\lambda = 0.50$ for La and 0.71 for Hg. This is qualitatively consistent with the experimental observation that Hg ($T_c = 98$ K) is higher than La ($T_c = 39$ K)^{37,38}.

To investigate how U_M affects λ in more detail, we perform calculations by rescaling U_M hypothetically. We plot λ as a function of $U^{x^2-y^2}$ in Fig. 4. In the calculation, \hat{H}_M^0 and the ratio between all the elements of U_M are fixed. We see that λ increases rapidly with smaller $U^{x^2-y^2}$ and plateaus with larger $U^{x^2-y^2}$ in both materials. The cases of original $U^{x^2-y^2}$ as shown in table II are shown by open circles. These are in the plateau region⁷¹. Because of the small changes in the region, λ of the two cuprates do not change so much even if we use U_m instead of U_M , where $\lambda_{\text{cRPA}}^{\text{La}} = 0.52$ and $\lambda_{\text{cRPA}}^{\text{Hg}} = 0.64$. The difference between La and Hg is mainly from the hybridization of the $d_{x^2-y^2}$ orbital with the d_{z^2} orbital. This is already examined by previous FLEX calculations with empirically determined interaction parameters³⁹. Sakakibara *et al.* already showed that FLEX reproduces the experimental trends of T_c (see Fig. 1(a) of Ref. 42). The detailed mechanism how the hybridization affects T_c was discussed in Sec. III D of Ref. 40.

V. SUMMARY

With mRPA, we obtain the two-orbital Hubbard models for La_2CuO_4 and $\text{HgBa}_2\text{CuO}_4$ in first-principles. The main part of mRPA is how to determine the on-site interaction parametrized by four parameters. We see that the interactions are close to those in cRPA. However, we see some differences. A difference comes from the fact that the effective size of the polarization function P_m in cRPA becomes smaller than P_M in mRPA. This is because that the probability factors c_i in Eq. (8) are distributed among the oxygen bands when d - p hybridization is strong, as in $\text{HgBa}_2\text{CuO}_4$.

For the models, we perform FLEX to evaluate superconductivity. The results are consistent with experi-

ments. With the interaction obtained in mRPA, we confirm that T_c is not so strongly dependent on the scale of interaction. Along the line of the combination of mRPA and FLEX, we will be able to predict new superconductors.

We appreciate discussions with Drs. Friedlich, Şaşıoğlu, Imada, Arita, Hirayama, Kuroki, S. W. Jang, and M. J. Han. H.S. appreciates fruitful discussions with Drs. Misawa, Nomura, and Shinaoka. This work was supported by JSPS KAKENHI (Grant No. 16K21175, 17K05499). The computing resource is supported by Computing System for Research in Kyushu University (ITO system), the supercomputer system in RIKEN (HOKUSAI), and the supercomputer system in ISSP (sekirei).

-
- * sakakibara.tottori.u@gmail.com
- ¹ C. Honerkamp, Phys. Rev. B **85**, 195129 (2012).
 - ² M. Kinza and C. Honerkamp, Phys. Rev. B **92**, 045113 (2015).
 - ³ S. R. White, Phys. Rev. Lett. **69**, 2863 (1992).
 - ⁴ E. Gull, A. J. Millis, A. I. Lichtenstein, A. N. Rubtsov, M. Troyer, and P. Werner, Rev. Mod. Phys. **83**, 349 (2011).
 - ⁵ D. Ceperley, G. V. Chester, and M. H. Kalos, Phys. Rev. B **16**, 3081 (1977).
 - ⁶ A. Georges, G. Kotliar, W. Krauth, and M. J. Rozenberg, Rev. Mod. Phys. **68**, 13 (1996).
 - ⁷ Y.M. Vilks and A.-M.S. Tremblay, J. Phys. I France **7**, 1309 (1997).
 - ⁸ B. Kyung, J.-S. Landry, and A.-M. S. Tremblay, Phys. Rev. B **68**, 174502 (2003).
 - ⁹ S. Onari and H. Kontani, Phys. Rev. Lett. **109**, 137001 (2012).
 - ¹⁰ M. Tsuchiizu, Y. Yamakawa, S. Onari, Y. Ohno, and H. Kontani, Phys. Rev. B **91**, 155103 (2015).
 - ¹¹ N. E. Bickers, D. J. Scalapino, and S. R. White, Phys. Rev. Lett. **62**, 961 (1989).
 - ¹² H. Sakakibara, S. W. Jang, H. Kino, M. J. Han, K. Kuroki, and T. Kotani, J. Phys. Soc. Jpn. **86**, 044714 (2017).
 - ¹³ N. Marzari and D. Vanderbilt, Phys. Rev. B **56**, 12847 (1997).
 - ¹⁴ I. Souza, N. Marzari, and D. Vanderbilt, Phys. Rev. B **65**, 035109 (2001).
 - ¹⁵ T. Kotani, J. Phys. Condens. Matter **12**, 2413 (2000).
 - ¹⁶ F. Aryasetiawan, M. Imada, A. Georges, G. Kotliar, S. Biermann, and A. I. Lichtenstein, Phys. Rev. B **70**, 195104 (2004).
 - ¹⁷ K. Nakamura, R. Arita, and M. Imada, J. Phys. Soc. Jpn. **77**, 093711 (2008).
 - ¹⁸ K. Nakamura, Y. Yoshimoto, T. Kosugi, R. Arita, and M. Imada, J. Phys. Soc. Jpn. **78**, 083710 (2009).
 - ¹⁹ T. Miyake, F. Aryasetiawan, and M. Imada, Phys. Rev. B **80**, 155134 (2009).
 - ²⁰ T. Miyake, K. Nakamura, R. Arita, and M. Imada, J. Phys. Soc. Jpn. **79**, 044705 (2010).
 - ²¹ K. Nakamura, Y. Yoshimoto, Y. Nohara, and M. Imada, J. Phys. Soc. Jpn. **79**, 123708 (2010).
 - ²² T. O. Wehling, E. Şaşıoğlu, C. Friedrich, A. I. Lichtenstein, M. I. Katsnelson, and S. Blügel, Phys. Rev. Lett. **106**, 236805 (2011).
 - ²³ E. Şaşıoğlu, C. Friedrich, and S. Blügel, Phys. Rev. B **83**, 121101 (2011).
 - ²⁴ T. Misawa, K. Nakamura, and M. Imada, Phys. Rev. Lett. **108**, 177007 (2012).
 - ²⁵ Y. Nomura, M. Kaltak, K. Nakamura, C. Taranto, S. Sakai, A. Toschi, R. Arita, K. Held, G. Kresse, and M. Imada, Phys. Rev. B **86**, 085117 (2012).
 - ²⁶ K. Nakamura, Y. Yoshimoto, and M. Imada, Phys. Rev. B **86**, 205117 (2012).
 - ²⁷ H. Shinaoka, T. Misawa, K. Nakamura, and M. Imada, J. Phys. Soc. Jpn. **81**, 034701 (2012).
 - ²⁸ P. Werner, M. Casula, T. Miyake, F. Aryasetiawan, A. J. Millis, and S. Biermann, Nat. Phys. **8**, 331 (2012).
 - ²⁹ M. Casula, P. Werner, L. Vaugier, F. Aryasetiawan, T. Miyake, A. J. Millis, and S. Biermann, Phys. Rev. Lett. **109**, 126408 (2012).
 - ³⁰ T. Misawa and M. Imada, Nat. Commun. **5**, 6738 (2014).
 - ³¹ T. Koretsune and C. Hotta, Phys. Rev. B **89**, 045102 (2014).
 - ³² E. Şaşıoğlu, in *Lecture Notes of the 45th IFF Spring School Computing Solids - Models, ab initio methods and supercomputing* (Forschungszentrum Jülich, 2014).
 - ³³ H. Shinaoka, M. Troyer, and P. Werner, Phys. Rev. B **91**, 245156 (2015).
 - ³⁴ S. W. Jang, H. Sakakibara, H. Kino, T. Kotani, K. Kuroki, and M. J. Han, Sci. Rep. **6**, 33397 (2016).
 - ³⁵ A. van Roekeghem, L. Vaugier, H. Jiang, and S. Biermann, Phys. Rev. B **94**, 125147 (2016).
 - ³⁶ M. Hirayama, Y. Yamaji, T. Misawa, and M. Imada, Phys. Rev. B **98**, 134501 (2018).
 - ³⁷ H. Takagi, R. J. Cava, M. Marezio, B. Batlogg, J. J. Krajewski, W. F. Peck, P. Bordet, and D. E. Cox, Phys. Rev. Lett. **68**, 3777 (1992).
 - ³⁸ A. Yamamoto, K. Minami, W.-Z. Hu, A. Miyakita, M. Izumi, and S. Tajima, Phys. Rev. B **65**, 104505 (2002).
 - ³⁹ H. Sakakibara, H. Usui, K. Kuroki, R. Arita, and H. Aoki, Phys. Rev. Lett. **105**, 057003 (2010).
 - ⁴⁰ H. Sakakibara, H. Usui, K. Kuroki, R. Arita, and H. Aoki, Phys. Rev. B **85**, 064501 (2012).
 - ⁴¹ H. Sakakibara, K. Suzuki, H. Usui, K. Kuroki,

- R. Arita, D. J. Scalapino, and H. Aoki, Phys. Rev. B **86**, 134520 (2012).
- ⁴² H. Sakakibara, K. Suzuki, H. Usui, S. Miyao, I. Maruyama, K. Kusakabe, R. Arita, H. Aoki, and K. Kuroki, Phys. Rev. B **89**, 224505 (2014).
- ⁴³ H. Kamimura and M. Eto, J. Phys. Soc. Jpn. **59**, 3053 (1990).
- ⁴⁴ M. Eto and H. Kamimura, J. Phys. Soc. Jpn. **60**, 2311 (1991).
- ⁴⁵ A. Freeman and J. Yu, Physica B+C **150**, 50 (1988).
- ⁴⁶ X. Wang, H. T. Dang, and A. J. Millis, Phys. Rev. B **84**, 014530 (2011).
- ⁴⁷ L. Hozoi, L. Siurakshina, P. Fulde, and J. van den Brink, Sci. Rep. **1**, 65 (2011).
- ⁴⁸ S. Uebelacker and C. Honerkamp, Phys. Rev. B **85**, 155122 (2012).
- ⁴⁹ L. Hozoi and M. S. Laad, Phys. Rev. Lett. **99**, 256404 (2007).
- ⁵⁰ C. E. Matt, D. Sutter, A. M. Cook, Y. Sassa, M. Månsson, O. Tjernberg, L. Das, M. Horio, D. Destraz, C. G. Fatuzzo, K. Hauser, M. Shi, M. Kobayashi, V. N. Strocov, T. Schmitt, P. Dudin, M. Hoesch, S. Pyon, T. Takayama, H. Takagi, O. J. Lipscombe, S. M. Hayden, T. Kurosawa, N. Momono, M. Oda, T. Neupert, and J. Chang, Nature Communications **9**, 972 (2018).
- ⁵¹ J. D. Jorgensen, H. B. Schüttler, D. G. Hinks, D. W. Capone II, K. Zhang, M. B. Brodsky, and D. J. Scalapino, Phys. Rev. Lett. **58**, 1024 (1987).
- ⁵² J. Wagner, P. Radaelli, D. Hinks, J. Jorgensen, J. Mitchell, B. Dabrowski, G. Knapp, and M. Beno, Physica C: Superconductivity **210**, 447 (1993).
- ⁵³ A first-principles electronic-structure suite based on the PMT method, `ecalj` package, is freely available from <https://github.com/tkotani/ecalj>. Its one-body part is developed based on the LMTO part in the LMsuit package at <http://www.lmsuite.org/>.
- ⁵⁴ T. Kotani, M. van Schilfgaarde, and S. V. Faleev, Phys. Rev. B **76**, 165106 (2007).
- ⁵⁵ T. Kotani, J. Phys. Soc. Jpn. **83**, 094711 (2014).
- ⁵⁶ D. Deguchi, K. Sato, H. Kino, and T. Kotani, Jpn. J. Appl. Phys. **55**, 051201 (2016).
- ⁵⁷ In our previous paper¹², we made a wrong statement that U_M would become smaller if we consider off-site interactions.
- ⁵⁸ We use the tetrahedron method^{54,55} in the Brillouin zone to calculate the matrix W and U_m , where we use $8 \times 8 \times 8(8 \times 8 \times 4)$ k -points for $\text{La}_2\text{CuO}_4(\text{HgBa}_2\text{CuO}_4)$. For a model calculation to determine $U_M^{122'1'}$, we take $64 \times 64 \times 4$ k -point grids for discrete summation. We use dense enough 4096 Matsubara meshes at $T = 0.005$ eV (virtually equal to $T = 0$ eV.).
- ⁵⁹ Y. Ohta, T. Tohyama, and S. Maekawa, Phys. Rev. B **43**, 2968 (1991).
- ⁶⁰ O. Andersen, A. Liechtenstein, O. Jepsen, and F. Paulsen, Journal of Physics and Chemistry of Solids **56**, 1573 (1995), proceedings of the Conference on Spectroscopies in Novel Superconductors.
- ⁶¹ E. Pavarini, I. Dasgupta, T. Saha-Dasgupta, O. Jepsen, and O. K. Andersen, Phys. Rev. Lett. **87**, 047003 (2001).
- ⁶² M. Mori, G. Khaliullin, T. Tohyama, and S. Maekawa, Phys. Rev. Lett. **101**, 247003 (2008).
- ⁶³ C. Weber, K. Haule, and G. Kotliar, Phys. Rev. B **82**, 125107 (2010).
- ⁶⁴ C. Weber, C. Yee, K. Haule, and G. Kotliar, Europhys. Lett. **100**, 37001 (2012).
- ⁶⁵ A. I. Liechtenstein and M. I. Katsnelson, Phys. Rev. B **57**, 6884 (1998).
- ⁶⁶ K. Yada and H. Kontani, J. Phys. Soc. Jpn. **74**, 2161 (2005).
- ⁶⁷ M. Mochizuki, Y. Yanase, and M. Ogata, Phys. Rev. Lett. **94**, 147005 (2005).
- ⁶⁸ T. Takimoto, T. Hotta, and K. Ueda, Phys. Rev. B **69**, 104504 (2004).
- ⁶⁹ H. Ikeda, R. Arita, and J. Kuneš, Phys. Rev. B **81**, 054502 (2010).
- ⁷⁰ K. Kuroki, H. Usui, S. Onari, R. Arita, and H. Aoki, Phys. Rev. B **79**, 224511 (2009).
- ⁷¹ The correlation between U/t and T_c is discussed with Hubbard model calculations, e.g., in Ref.⁷².
- ⁷² H. Yokoyama, M. Ogata, Y. Tanaka, K. Kobayashi, and H. Tsuchiura, J. Phys. Soc. Jpn. **82**, 014707 (2013).